Application of a homogenous membrane potential assay to assess mitochondrial function

Srilatha Sakamuru, Xiao Li, Matias S. Attene-Ramos, Ruili Huang, Jianming Lu, Louie Shou, Min Shen, Raymond R. Tice, Christopher P. Austin and Menghang Xia

Physiol. Genomics 44:495-503, 2012. First published 20 March 2012;
doi:10.1152/physiolgenomics.00161.2011

Physiol Genomics 44: 495–503, 2012.
First published March 20, 2012; doi:10.1152/physiolgenomics.00161.2011.

CALL FOR PAPERS | *Mitochondrial Metabolism*

Application of a homogenous membrane potential assay to assess mitochondrial function

Srilatha Sakamuru,[1]* Xiao Li,[2]* Matias S. Attene-Ramos,[1] Ruili Huang,[1] Jianming Lu,[3] Louie Shou,[1] Min Shen,[1] Raymond R. Tice,[4] Christopher P. Austin,[1] and Menghang Xia[1]

[1]*NIH Chemical Genomics Center, National Institutes of Health, Bethesda;* [2]*BD Diagnostics - Diagnostic Systems, Sparks;* [3]*Codex Biosolutions, Montgomery Village, Maryland; and* [4]*Division of the National Toxicology Program, National Institute of Environmental Health Sciences, Research Triangle Park, North Carolina*

Submitted 9 November 2011; accepted in final form 19 March 2012

Sakamuru S, Li X, Attene-Ramos MS, Huang R, Lu J, Shou L, Shen M, Tice RR, Austin CP, Xia M. Application of a homogenous membrane potential assay to assess mitochondrial function. *Physiol Genomics* 44: 495–503, 2012. First published March 20, 2012; doi:10.1152/physiolgenomics.00161.2011.—Decreases in mitochondrial membrane potential (MMP) have been associated with mitochondrial dysfunction that could lead to cell death. The MMP is generated by an electrochemical gradient via the mitochondrial electron transport chain coupled to a series of redox reactions. Measuring the MMP in living cells is commonly used to assess the effect of chemicals on mitochondrial function; decreases in MMP can be detected using lipophilic cationic fluorescent dyes. To identify an optimal dye for use in a high-throughput screening (HTS) format, we compared the ability of mitochondrial membrane potential sensor (Mito-MPS), 5,5′,6,6′-tetrachloro-1,1′,3,3′ tetraethylbenzimidazolylcarbocyanine iodide, rhodamine 123, and tetramethylrhodamine to quantify a decrease in MMP in chemically exposed HepG2 cells cultured in 1,536-well plates. Under the conditions used, the optimal dye for this purpose is Mito-MPS. Next, we developed and optimized a homogenous cell-based Mito-MPS assay for use in 1,536-well plate format and demonstrated the utility of this assay by screening 1,280 compounds in the library of pharmacologically active compounds in HepG2 cells using a quantitative high-throughput screening platform. From the screening, we identified 14 compounds that disrupted the MMP, with half-maximal potencies ranging from 0.15 to 18 μM; among these, compound clusters that contained tyrphostin and 3′-substituted indolone analogs exhibited a structure-activity relationship. Our results demonstrate that this homogenous cell-based Mito-MPS assay can be used to evaluate the ability of large numbers of chemicals to decrease mitochondrial function.

Mito-MPS; mitochondrial membrane potential assay; quantitative high-throughput screening; 1,536-well plate

MITOCHONDRIA ARE INTRACELLULAR organelles that play a vital role in cellular metabolism, including heme, fatty acid, and steroid synthesis; oxidative phosphorylation; Ca^{2+} homeostasis; and apoptosis (15, 24). Mitochondria are enclosed within an outer and inner membrane. The inner membrane is more complex in structure, and contains the electron transport chain (ETC) complex and the complex for ATP synthesis (1). The majority of ATP in eukaryotic cells is produced in mitochondria through oxidative phosphorylation. This process consists of a series of redox reactions in which electrons are transferred from electron donors to electron acceptors. The energy released by electrons flowing through the ETC transports protons across the inner membrane, creating an electrochemical gradient. The electrochemical gradient consists of two parts, the electric potential and the proton gradient. This electrochemical gradient drives the synthesis of ATP (20). The mitochondrial membrane potential (MMP, $\Delta\psi m$) is generated by the electric potential across the inner mitochondrial membrane. Measuring the MMP is useful for evaluating mitochondrial function (21). A decrease in MMP can be induced by xenobiotics that dissipate the MMP directly (uncouple) or by xenobiotics that disrupt other cellular processes or affect different mitochondrial functions including respiration, the tricarboxylic acid (TCA) cycle, fatty acid β-oxidation, and pyruvate or fatty acid uptake. A decrease in the MMP may also be linked to apoptosis pathways because depolarization of the mitochondrial membrane opens the mitochondrial permeability transition pore, which may lead to the release of apoptosis initiation factors, such as cytochrome c, and trigger the apoptosis cascade (19, 33, 37).

Several cell-based MMP assays are available that use membrane-permeable fluorescent cationic dyes, such as 3,3′-diehexiloxadicarbocyanine iodide (DiOC6) (27), rhodamine-123 (28), chloromethyl-tetramethyl-rosamine (MitoTracker Orange) (32), tetramethylrhodamine methyl ester (TMRM) (28), and tetramethylrhodamine ethyl ester (TMRE) (28), to determine a reduction in MMP quantitatively. These dyes distribute electrophoretically into the mitochondrial matrix in response to the electrical potential across the inner mitochondrial membrane and, upon accumulation, exhibit a red shift in both their excitation and emission spectra. However, most of these assays have limitations, including low sensitivity, high cytotoxicity, and specific inhibition of mitochondrial functions (29); the potential of being pumped out of mitochondria by multidrug resistance pumps (6); or the need for multiple wash steps with long equilibrium time.

Another fluorescent lipophilic cationic dye, 5,5′,6,6′-tetrachloro-1,1′,3,3′-tetraethylbenzimidazolo carbocyanine iodide (JC-1), was developed for measurement of the MMP (25). JC-1 is specific and sensitive to reduction in the MMP, but it is poorly water soluble and has a low signal-to-background (S/B) window (17). To overcome these limitations, we developed a homogenous cell-based assay with a water-soluble mitochondrial membrane potential sensor (Mito-MPS), a modified ver-

* S. Sakamuru and X. Li contributed equally to this work.

Address for reprint requests and other correspondence: M. Xia, National Institutes of Health, National Center for Advancing Translational Sciences, NIH Chemical Genomics Center, 9800 Medical Center Dr., Bethesda, MD 20892-3370.

sion of JC-1 with similar fluorescent properties and subcellular staining patterns, to quantify MMP. Figure 1 illustrates the principle of this assay.

In the present study, we first compared the ability of Mito-MPS, JC-1, rhodamine 123, and TMRE to quantify chemically induced reductions in MMP. Next, we optimized and miniaturized the cell-based Mito-MPS assay for use in 1,536-well plate format and demonstrated the utility of this homogenous assay by screening the LOPAC (Library of Pharmacologically Active Compounds) collection of 1,280 compounds in a quantitative high-throughput screening (qHTS) format. We identified several compounds that significantly reduced the MMP and confirmed their activity using a high-content imager. We show that this assay is highly reliable and easy to run in 1,536-well plate format, indicating that this assay can be used for screening large compound libraries.

MATERIALS AND METHODS

Cell culture. Human HepG2 (hepatocellular carcinoma) cells (12) were purchased from the American Type Culture Collection (ATCC, Manassas, VA). These cells were cultured in Eagle's minimum essential medium (ATCC) supplemented with 10% FBS (Hyclone Laboratories, Logan, UT), 50 U/ml penicillin, and 50 μg/ml streptomycin (Invitrogen, Carlsbad, CA). The cells were maintained at 37°C under a humidified atmosphere and 5% CO_2.

Reagents. The Mito-MPS was obtained from BD Biosciences (Rockville, MD). Mito-MPS is equivalent to mitochondrial membrane potential indicator (m-MPI), purchased from Codex Biosolutions (Montgomery Village, MD). JC-1, rhodamine 123, and TMRE were purchased from Invitrogen.

A library of pharmacologically active compounds (LOPAC), containing 1,280 compounds with known pharmacological activity, was purchased from Sigma-Aldrich (St. Louis, MO), as was FCCP (mesoxalonitrile 4-trifluoromethoxyphenylhydrazone), antimycin A, apigenin, (2′Z,3′E)-6-bromoindirubin-3′-oxime (BIO), diphenyleneiodonium chloride, 2,4-dinitrophenol (DNP), genistein, GW-5074, indirubin-3′-oxime, isoliquiritigenin, niclosamide, piceatannol, rotenone, rottlerin, SP-600125, tyrphostin A9, and Tyrphostin AG-879. Tyrphostin 47 was purchased from Cayman Chemical (Ann Arbor, MI).

Cell-based MMP assay using different dyes. JC-1, Mito-MPS, rhodamine 123, and TMRE were tested in cell-based MMP assays. Briefly, HepG2 cells were dispensed at 8,000 cells/25 μl/well in poly-D-lysine coated 384-well black-clear plates (BD Biosciences, Bedford, MA). After the plates were incubated at 37°C overnight, the culture medium was removed from each well, and 25 μl of assay buffer containing different concentrations of FCCP, rotenone, or antimycin were added into each well. The plates were incubated at 37°C for 1 h, followed by the addition of 25 μl of 2× dye solutions. The final concentrations for JC-1 and Mito-MPS were 10 μM and for rhodamine 123 (2) and TMRE (7) were 500 nM. The plates were incubated at 37°C with the dyes for another 30 min and then washed with assay buffer. Fluorescence intensities (485 nm excitation, and 535 and 590 nm emissions for JC-1 and Mito-MPS; 507 nm excitation and 529 nm emission for rhodamine; 549 nm excitation and 574 nm emission for TMRE) were measured using a SpectraMax Gemini EM plate reader (Molecular Devices, Sunnyvale, CA).

Cell-based Mito-MPS assay and qHTS. The protocol of Mito-MPS assay in a 1,536-well plate format is described in Table 1. Briefly, HepG2 cells were suspended in culture medium and dispensed at 2,000 cells/5 μl/well in tissue culture treated 1,536-well black-clear bottom assay plates (Greiner Bio-One North America) using a Flying Reagent Dispenser (FRD) (Aurora Discovery). The assay plates were incubated at 37°C overnight to allow the cells to attach to the wells. The next day, 23 nl of compounds at various concentrations or dimethyl sulfoxide (DMSO; Fisher Scientific, Pittsburgh, PA) control was transferred to the assay plate via a pin tool (Kalypsys, San Diego, CA). The final concentration of the compounds in the 5 μl assay volume ranged from 0.6 nM to 46 μM. The positive control plate format was as follows: *Column 1*, FCCP, an uncoupler of mitochondrial oxidative phosphorylation (10), ranging from 1.4 to 11.5 μM; *column 2*, 9.2 μM FCCP; *column 3*, 6.9 μM (wells 1–16) and 3.45 μM (wells 17–32) FCCP; *column 4*, DMSO only; and *columns 5–48*, compounds. The plates were incubated for 1 or 5 h at 37°C, followed by the addition of 5 μl of 2× dye-loading solution into each well using the FRD. And then, these assay plates were incubated at 37°C for 30 min. Fluorescence intensity (490 nm excitation and 535 nm emission for monomer; and 540 nm excitation and 590 nm emissions for aggregates) was measured using an EnVision plate reader (PerkinElmer, Shelton, CT). Data were expressed as the ratio of 590 nm/535 nm emissions.

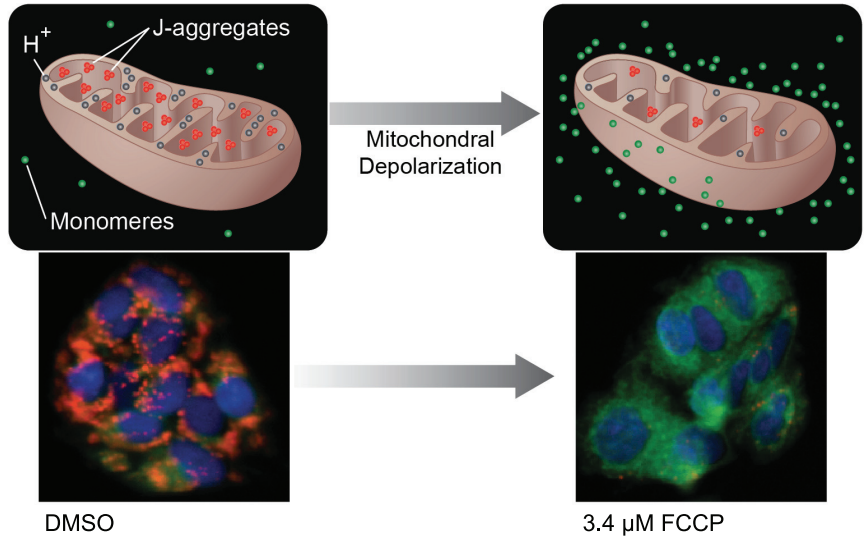

Fig. 1. Principle of the mitochondrial membrane potential sensor (Mito-MPS) assay. Based on the molecule structure of 5,5′,6,6′-tetrachloro-1,1′,3,3′-tetraethylbenzimidazolo carbocyanine iodide (JC-1), Mito-MPS was modified to be more water soluble. In healthy cells (*left*, DMSO control), the mitochondria are polarized and Mito-MPS accumulates in the mitochondria as aggregates with red fluorescence (emission at 590 nm). In cells with lower mitochondrial membrane potential [MMP, *right*, 3.4 μM mesoxalonitrile 4-trifluoromethoxyphenylhydrazone (FCCP) treated], Mito-MPS remains in cytoplasm as the monomeric form that shows green fluorescence (emission at 535 nm). The dye undergoes a change in fluorescence emission from green to red when the MMP increases or vice versa. This process is reversible. The red/green ratio can be used to determine the mitochondrial function of the cells (25).

Table 1. *Quantitative high-throughput screening protocol*

Step	Parameter	Value	Description
1	plate cells	5 μl	2,000 HepG2 cells
2	incubation time	overnight (18 h)	cells adhere and acclimate
3	library compound	23 nl	2.9 nM–46 μM titration series
	control positive compound	23 nl	17.5 nM–11.5 μM titrations (FCCP)
4	incubation time	1 h or 5 h	compound treatment
5	reagent	5 μl	Mito-MPS dye
6	incubation time	30 min	
7	assay readout	Ex/Em = 485/535 nm Ex/Em = 540/590 nm	envision plate reader

1, Black clear bottom 1,536-well plates, single tip dispense of 2,000 cells/well into all wells; *2*, 37°C, 5% CO_2 incubator; *3*, Pin tool transfer of library to columns 5–48, and controls to columns 1–4; *4*, 37°C, 5% CO_2 incubator; *5*, Single tip dispense of 5 μl of Mito-MPS dye; *6*, 37°C, 5% CO_2 incubator; *7*, Green monomers: excitation (Ex): 485 nm; emission (Em): 535 nm and J-aggregates: Ex: 540 nm; Em: 590 nm.

In the confirmation study, the selected active compounds were retested in 24 point titrations with concentrations ranging from 5.5 pM to 46 μM in the Mito-MPS assay using the same protocol as described above except 24 point titrations were within the same 1,536-well plate.

Imaging-based MMP assay. HepG2 cells were dispensed at 2,000 cells/5 μl/well in tissue culture-treated 1,536-well black-clear bottom assay plates (Greiner Bio-One North America) using an FRD (Aurora Discovery). After being cultured overnight at 37°C, the assay plates were treated with the compounds at 37°C for 1 or 5 h, followed by addition of 5 μl of m-MPI reagent (Codex) with 0.3 μg/ml of Hoechst 33342 (Invitrogen) used to stain DNA. The plates were incubated for 30 min at 37°C. The fluorescence intensities (482 nm excitation and 536 nm emission for green fluorescent monomers; 543 nm excitation and 593 nm emission for red fluorescent aggregates; 377 nm excitation and 447 nm emission for Hoechst 33342) were measured using an ImageXpress Micro Widefield High Content Screening System (Molecular Devices, Sunnyvale, CA). Imaging was processed and analyzed with the MetaXpress and PowerCore software (MDC) using the Multi Wavelength Cell Scoring algorithm. The mean of average fluorescence intensity from each positive cell was calculated per well for both green and red fluorescent colors. Data were expressed as the ratio of 593 nm/536 nm emissions.

Cell viability assay. Cell viability after compound treatment was measured using a luciferase-coupled ATP quantitation assay (CellTiter-Glo viability assay; Promega, Madison, WI), in which the total amount of ATP in a well correlates with the number of viable cells present. The cells were dispensed at 2,000 cells/5 μl/well in 1,536-well white/solid-bottom assay plates using an FRD. After the cells were incubated overnight at 37°C, 23 nl of the compounds at various concentrations was added into the plates using the pin tool. The assay plates were incubated for 1 or 5 h at 37°C, followed by the addition of 5 μl/well of CellTiter-Glo reagent. After a 30 min incubation at room temperature, the luminescence intensity of the plates was measured using a ViewLux plate reader (PerkinElmer).

Data analysis. Primary data analysis was performed as previously described (36). Briefly, raw plate reads for each titration point were first normalized relative to FCCP control (3.5 μM for 1 h and 6.9 μM for 5 h, 100%) and DMSO-only wells (basal, 0%) and then corrected by applying a pattern correction algorithm using compound-free control plates (DMSO plates). Concentration-response titration points for each compound were fitted to the Hill equation, yielding concentrations of half-maximal inhibition (IC_{50}) and maximal response (efficacy) values.

Compounds considered to be active in the Mito-MPS assay showed inhibition in the 590 nm and in the ratiometric readings, and had an $IC_{50} < 20$ μM in the ratiometric reading at either the 1 or 5 h treatment. A subset of active compounds selected based on potency, novelty, and structure-activity relationship was ordered from commercial vendors for confirmation and follow-up studies.

RESULTS

Evaluation of membrane potential fluorescent dyes in MMP assay. Based on the JC-1 structure, a water-soluble Mito-MPS dye was developed by Lu et al. (17) to measure reduction in MMP. To identify the optimal dye for assessing the MMP in an HTS format, we compared Mito-MPS with JC-1, rhodamine 123, and TMRE. Three known mitochondrial inhibitors, FCCP (10), rotenone (8), and antimycin A (31), were tested in the MMP assays using these four dyes. A decrease in MMP was measured in HepG2 cells after compound treatment for 1 h. Among these dyes, Mito-MPS had the best S/B ratio compared with the others (Fig. 2). The maximum S/B of DMSO control over FCCP, rotenone, or antimycin treatment was 11- to 20-fold in Mito-MPS assay, but only two- to threefold in MMP assays using JC-1, rhodamine 123, or TMRE. These results indicate that the Mito-MPS dye is superior to JC-1, rhodamine 123, and TMRE for the MMP assay. The AC_{50} (concentration of half-maximal activation) values of fold change for FCCP, rotenone, and antimycin in the Mito-MPS assay were 0.59, 24.1, and 2.54, μM, respectively.

Optimization and validation of the cell-based Mito-MPS assay in 1,536-well plate format. To optimize the Mito-MPS assay in a 1,536-well plate format, we first modified the Mito-MPS assay into a homogenous format and tested four known mitochondrial inhibitors: rotenone, antimycin, DNP (22), and FCCP. All four compounds disrupted MMP in a concentration-dependent manner. Among these compounds, FCCP was the most potent with IC_{50} values of 1.31 and 1.44 μM after 1 and 5 h of treatment, respectively, followed by antimycin (1 h = 4.51 μM, 5 h = 3.73 μM), rotenone (1 h = 38.9 μM, 5 h = 19.9 μM), and DNP (1 h = 47.1 μM, 5 h = 50.6 μM) (Table 2). The rank orders of the compound potencies were same for 1 and 5 h of treatment (Table 2). The S/B ratios of these compounds ranged from three- to 30-fold. Antimycin and FCCP had higher S/B of 20- to 30-fold compared with DNP and rotenone. Thus, FCCP, a known MMP disrupter, was used as a control in the assay.

To evaluate the performance of the assay, DMSO plates were tested at 1 and 5 h in 1,536-well plate format. Because the FCCP concentration response curves were bell-shaped, due to the presence of cytotoxicity at high concentrations, three concentrations of FCCP (3.5, 6.9, and 9.2 μM) were used as positive controls in the experiment. After a 1 h treatment with DMSO or FCCP (Fig. 3*A*), the S/B ratios (value from DMSO

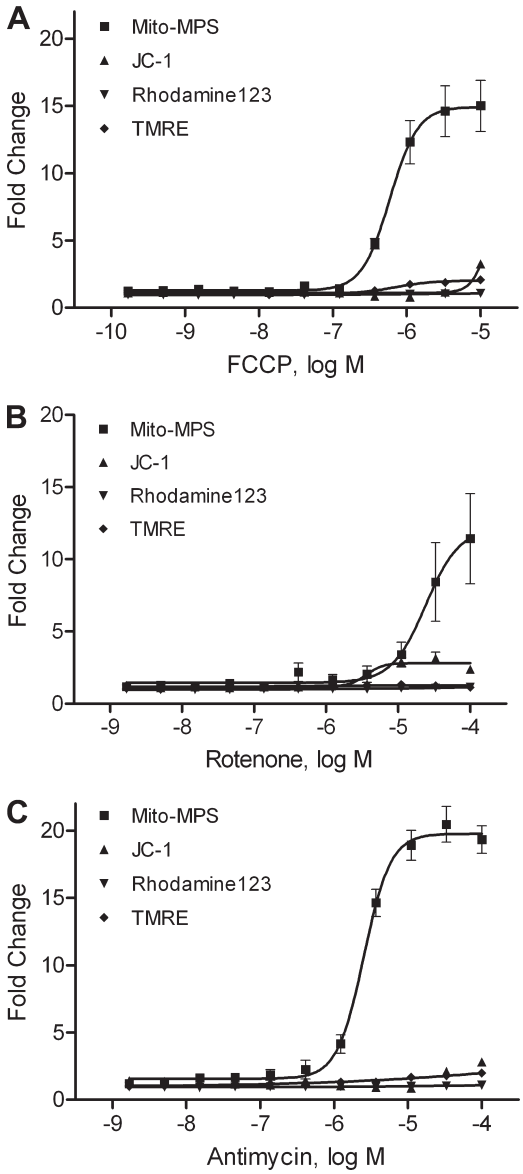

Fig. 2. Assay performance using MMP dyes, Mito-MPS, JC-1, rhodamine 123, or tetramethylrhodamine ethyl ester (TMRE). MMP was measured after the cells were treated with various concentrations of FCCP (*A*), rotenone (*B*), or antimycin (*C*) for 1 h in 384-well plate format. The fold change was defined as the value of DMSO control divided by the value of compound treatment. Values are means ± SD from 3 experiments performed in quadruplicate.

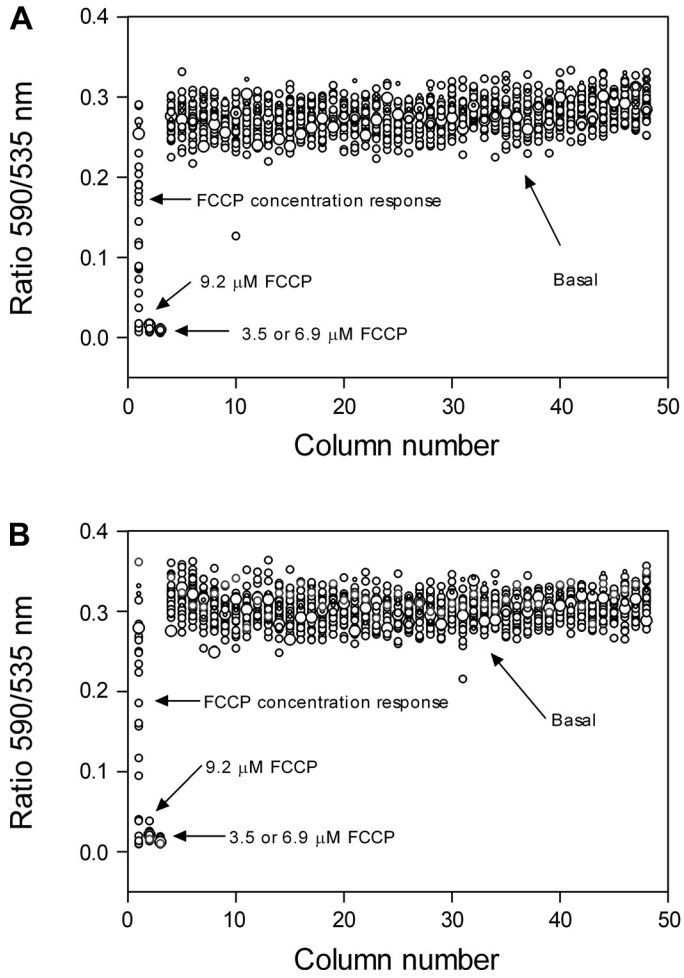

Fig. 3. Mito-MPS assay validation with DMSO plate. *Column 1* was a concentration response curve of FCCP in duplicate. *Column 2* was 9.2 μM FCCP. *Column 3* was 3.5 μM (*top* half) and 6.9 μM (*bottom* half) FCCP, respectively. *Columns 4–48* were treated with DMSO at a final concentration of 0.46%. Cells were treated with DMSO or FCCP for 1 h (*A*) or 5 h (*B*). Each value was expressed as the ratio of 590/535 nm emissions.

control/value from FCCP treatment) for 3.5, 6.9, and 9.2 μM FCCP were 37, 29, and 26, respectively; the coefficient of variation (CV) was 7.3%; and the Z′ factor (38) was 0.75. At 5 h, the S/B ratios for 3.5, 6.9, and 9.2 μM FCCP were 27, 20, and 16, respectively; the CV was 5.9%; and the Z′ factor was 0.78 (Fig. 3*B*). These results indicate that this Mito-MPS assay was robust and ready for high-throughput screening.

Identification of compounds that reduced MMP from LOPAC screening. To evaluate the performance of the Mito-MPS assay in qHTS, we screened the 1,280-compound LOPAC collection at 1 and 5 h in HepG2 cells. The concentration titration of FCCP was included as a positive control in each plate to examine data quality. After 1 or 5 h of treatment, the concentration response curves of FCCP from nine plates reproduced well with an average IC_{50} of 2.88 ± 0.43 μM, and

Table 2. *Activities of known mitochondria poison compounds in Mito-MPS assay*

Name	CASRN	IC_{50} (μM), 1 h	S/B, fold	IC_{50} (μM), 5 h	S/B, fold
Antimycin A	1397-94-0	4.51	24.7	3.73	30.5
DNP	51-28-5	47.1	3.12	50.6	5.55
FCCP	370-86-5	1.31	20.5	1.44	23.2
Rotenone	83-79-4	38.9	5.97	19.9	19.4

IC_{50}, concentration of half-maximal inhibition; CASRN, Chemical Abstracts Services Registry Number; FCCP, mesoxalonitrile 4-trifluoromethoxyphenylhydrazone; DNP, 2,4-dinitrophenol; S/B, signal to background.

Table 3. *Mito-MPS assay statistics from primary screen*

Time Point	FCCP Controls, μM	S/B, fold	CV, %	Z′ Factor
1 h	2.88 ± 0.43	14.7 ± 1.7	7.1 ± 0.8	0.69 ± 0.09
5 h	3.85 ± 0.44	28.8 ± 0.6	6.0 ± 0.5	0.79 ± 0.03

CV, coefficient of variation.

3.85 ± 0.44 μM, respectively (Table 3). The average S/B was 14.7 and 28.8, and the average CV (%) in DMSO-only plates and the plates with low concentrations of compound (0.37 μM or below) was 7.1 and 6.0 after 1 and 5 h of compound treatment, respectively (Table 3). The average Z′ factor was 0.69 and 0.79 for 1 and 5 h of compound treatment, respectively (Table 3).

In the LOPAC primary screen, 71 compounds with IC_{50} values of <20 μM and efficacy values >70% either at 1 or 5 h of treatment were identified. Among these compounds, 42 were cherry-picked and retested in the Mito-MPS assay. The IC_{50} values for these 42 compounds (Supplemental Table S1) at these two time points correlated well with an R of 0.94.[1] The activity of these compounds was confirmed at both treatment times, yielding a confirmation rate of 100%. There was a very good correlation (R = 0.93 at 1 h, R = 0.96 at 5 h) of IC_{50} values for these 42 compounds between the primary screen and the cherry-pick confirmation.

To evaluate the cytotoxicity of these compounds, a cell viability assay was used to measure intracellular ATP content after 1 or 5 h of compound treatment. Among these 42 compounds, nine compounds including NSC-95397 (IC_{50} = 12.38 μM and 14.43 μM at 1 and 5 h, respectively), sanguinarine chloride (IC_{50} = 19.19 μM and 9.10 μM at 1 and 5 h, respectively), and WIN-62577 (IC_{50} = 18.25 μM and 19.78 μM at 1 and 5 h, respectively) induced significant cytotoxicity at both sample times (Supplemental Table S1). These results suggest that the compound-induced reduction of MMP might be due to cytotoxicity. SU-5416 (IC_{50} = 2.47 μM) and thapsigargin (IC_{50} = 1.58 μM) were cytotoxic only after 5 h of treatment. The other 31 compounds did not induce cytotoxicity at concentrations up to 46 μM after either 1 or 5 h of treatment (Supplemental Table S1).

Confirmation of compounds that reduced MMP. To further confirm the inhibitory effect of compounds on MMP, 14 compounds (Table 4) were selected based on the potency from the cherry-pick confirmation study, the extent of cytotoxicity, and compound structure and then purchased from commercial vendors. The activities of all 14 compounds at 1 or 5 h of treatment were confirmed in the Mito-MPS assay with a 100% confirmation rate (Table 4). The IC_{50} values for these 14 compounds in the confirmation studies correlated well with those in the primary screen (R of 0.93 for 1 h and 0.95 for 5 h). The IC_{50} values for these 14 compounds at both sample times also correlated well with R of 0.96. These compounds were further evaluated in an MMP assay using a high-content imaging readout. Among these compounds, tyrphostin A9 remained the most potent with an IC_{50} value of 70 nM at 1 h and 110 nM at 5 h of treatment (Table 4). The ranking order of the compound potency measured using high-content imaging was similar to that tested using the fluorescence readout (Table 4). In addition, the cytotoxicity of these compounds was also re-evaluated after 1 or 5 h of treatment. None of these compounds were cytotoxic at concentrations up to 46 μM after 1 h of treatment. However, after 5 h of treatment, two of the 14 compounds, niclosamide and rottlerin, were cytotoxic with <50% maximum inhibition of cell viability. The other 12 compounds were not cytotoxic at concentrations up to 46 μM after 5 h of treatment. These data suggest that plate readouts in Mito-MPS assay could be a useful format for large-scale compound screens, while the imaging-based readouts could be a useful tool in confirmation studies to visually capture the compound effect on MMP.

In the primary screen, we found that 20 of the 21 tyrphostin analogs in the LOPAC library significantly reduced MMP at 1 and/or 5 h of treatment (Supplemental Table S2). In the follow-up studies, tyrphostin A9, tyrphostin AG-879, and tyrphostin 47 were retested and confirmed in Mito-MPS assays using both high-content imaging readout and fluorescence plate readout (Table 4 and Fig. 4). Tyrphostin A9 and tyrphostin

[1] The online version of this article contains supplemental material.

Table 4. *Compound potency (μM) in primary screen (Mito-MPS assay), powder compound confirmation (Mito-MPS assay), imaging confirmation, and cytotoxicity assay at 1 and 5 h of treatment*

		1 h				5 h			
Name	CASRN	Primary Screen	Confirmation	Cytotoxicity	Imaging Confirmation	Primary Screen	Confirmation	Cytotoxicity*	Imaging Confirmation
Apigenin	520-36-5	25.91	7.17 ± 1.34	inactive	4.06	4.60	12.68 ± 3.17	inactive	9.49
BIO	667463-62-9	0.09	0.23 ± 0.06	inactive	1.83	0.23	0.42 ± 0.05	inactive	1.94
Diphenyleneiodonium chloride	4673-26-1	3.26	15.46 ± 5.84	inactive	19.87	1.83	8.05 ± 6.91	inactive	9.74
Genistein	446-72-0	25.91	18.10 ± 4.10	inactive	7.74	7.94	18.76 ± 5.70	inactive	12.27
GW-5074	220904-83-6	7.30	6.43 ± 1.41	inactive	6.52	2.31	5.85 ± 2.07	inactive	7.74
Indirubin-3′-oxime	160807-49-8	0.25	0.44 ± 0.09	inactive	4.38	0.41	0.55 ± 0.12	inactive	4.35
Isoliquiritigenin	961-29-5	6.51	5.87 ± 1.88	inactive	3.88	3.66	10.24 ± 2.53	inactive	12.27
Niclosamide	50-65-7	0.41	0.72 ± 0.50	inactive	0.41	0.32	0.75 ± 0.46	1.12 (48%)	0.52
Piceatannol	10083-24-6	10.31	5.87 ± 1.41	inactive	5.81	5.17	8.64 ± 2.35	inactive	12.27
Rottlerin	82-08-6	6.51	5.65 ± 2.59	inactive	1.54	3.26	4.04 ± 0.82	1.78 (49%)	1.37
SP-600125	129-56-6	1.15	2.50 ± 0.88	inactive	24.64	1.63	2.52 ± 0.31	inactive	27.47
Tyrphostin 47	122520-86-9	12.59	7.38 ± 0.84	inactive	16.39	16.35	21.0 ± 4.15	inactive	54.8
Tyrphostin A9	10537-47-0	0.07	0.15 ± 0.06	inactive	0.07	0.04	0.18 ± 0.08	inactive	0.11
Tyrphostin AG-879	148741-30-4	0.51	2.22 ± 0.99	inactive	1.23	0.73	4.06 ± 1.99	inactive	1.73

BIO, (2′Z,3′E)-6-bromoindirubin-3′-oxime. *Efficacies are shown in parentheses.

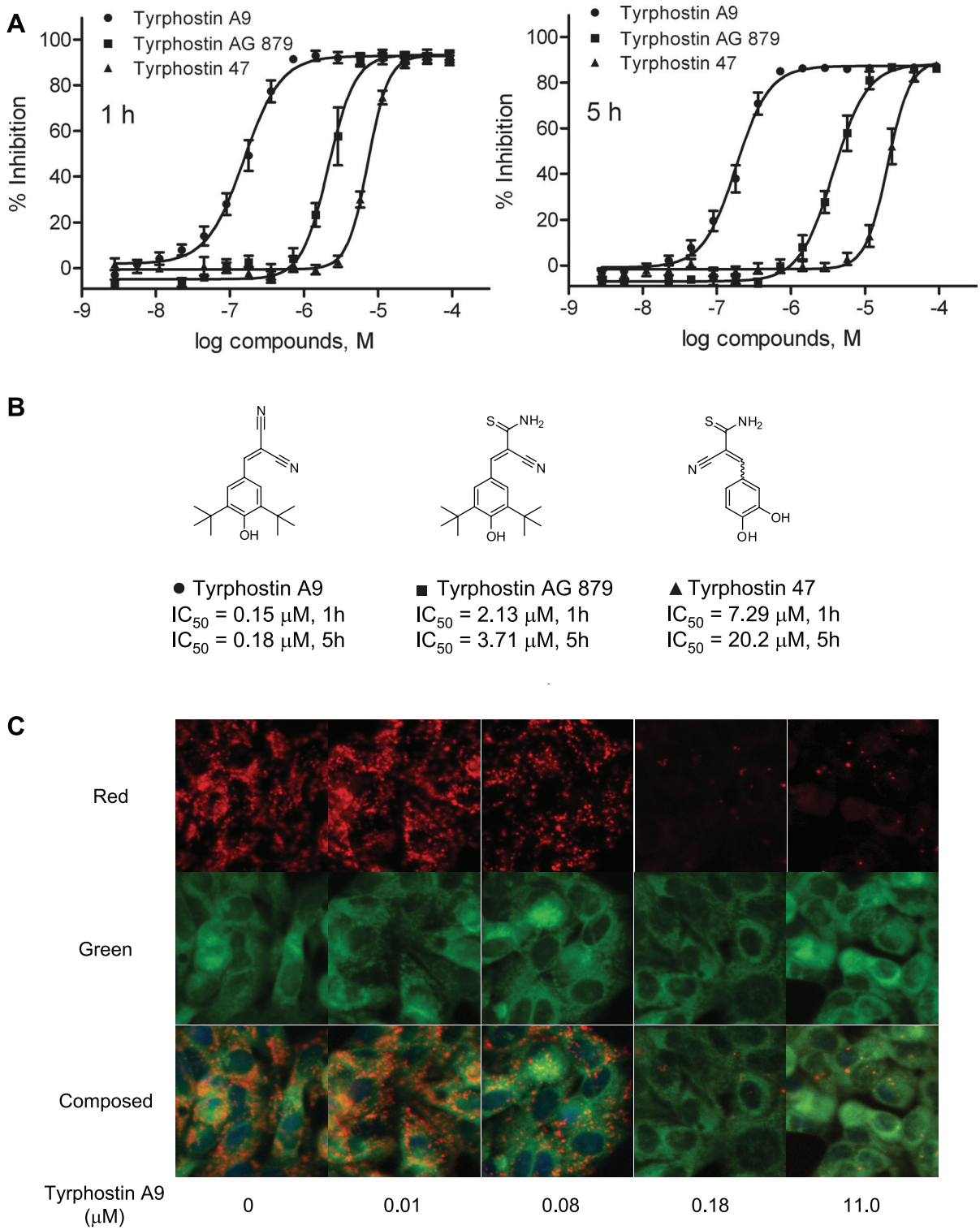

Fig. 4. Tyrphostin compounds. *A*: concentration response curves of tyrphostin A9, tyrphostin AG-879, and tyrphostin 47 in Mito-MPS assay at 1 h (*left*) or 5 h (*right*) of treatment. *B*: structures of these compounds are shown with compound names, half-maximal inhibition (IC_{50}) values in the Mito-MPS assay at 1 or 5 h of treatment. *C*: representative imagine of subcellular staining with Mito-MPS dye in the absence or in the presence of tyrphostin A9. Images acquired in ImageXpress microsystem using a ×20 objective. While red fluorescent aggregates are localized in the mitochondria, green fluorescent monomers are mainly in cytosol. The composed images were the merger of red and green fluorescence.

AG-879 were more potent than tyrphostin 47 (Fig. 4). From the results, we found that the potency of these compounds appeared to depend on the number of hydroxyl groups on the phenyl ring. Tyrphostin 47, which has two hydroxyl groups, was less potent than tyrphostin A9 and tyrphostin AG-879, each containing one hydroxyl group. Tyrphostin 25 and tyrphostin 51, each containing three hydroxyl groups on the phenyl ring, were inactive in the Mito-MPS assay at 1 h of treatment and showed weak activities at 5 h of treatment (Supplemental Table S2). The decreasing MMP of these compounds with increasing number of hydroxyl groups could result from reduced compound lipophilicity that leads to a reduced ability for the compounds to enter the cell. In addition, we found another group of compounds containing the 3-methyleneindolin-2-one (3′-substituted indolone) core structure that showed significant inhibitory effect on MMP. Three of these compounds, BIO, indirubin-3′-oxime, and GW-5074, reduced MMP in a concentration-dependent manner (Fig. 5). The other 3-methyleneindolin-2-one derivatives, such as IC261, SU-4312, SU-6656, SU-5416, and SU-9516, were also found to reduce MMP in the primary screen (Supplemental Table S3).

DISCUSSION

In eukaryote cells, mitochondria are central players in producing ATP, maintaining cellular homeostasis, and regulating cell death (35). Disruption of mitochondrial function by xenobiotics and drugs eventually leads to cell death (5). Evaluating chemically induced mitochondrial toxicity is thus a critical part in the evaluation of chemical toxicity. MMP is one of the most widely assessed parameters for mitochondrial toxicity. Changes in MMP are routinely measured using membrane-permeable fluorescent lipophilic cations, such as nonylacridine orange, safranine O, rhodamine 123, chloromethyl-tetramethyl-rosamine, and tetramethylrhodamine methyl and ethyl esters (TMRM and TMRE, respectively). In general, these lipophilic cationic dyes *1*) require a long time to achieve equilibrium distribution in the mitochondrial membrane; *2*) accumulate in membrane components other than the mitochondria (9); *3*) interfere with cell or mitochondrial metabolism (29); and *4*) have their cellular accumulation reduced by the multidrug resistance pump (6). DiOC6 (27), a fluorescent lipophilic cation, is also often used to measure changes in MMP and works effectively in isolated mitochondria. However, DiOC6 did not work well in cells because it detects both plasma and MMP changes (27). JC-1, a cyanine dye, has several advantages over rhodamines and other carbocyanines. This dye is more selective to mitochondria; its time to reach equilibrium is relatively short; it has a low background and minimal toxic effect on the mitochondrial electron transport chain (25). JC-1 accumulates in healthy mitochondria as aggregates but remains in the cytoplasm in the monomeric form in cells with lower MMP. However, the biggest limitation of JC-1 is its poor water solubility; the dye starts to precipitate in aqueous buffers at concentrations as low as 1 μM. Its poor water solubility makes it very difficult to load consistent amounts of JC-1 into cells, resulting in large experimental variations. JC-1 only works in certain types of cells,

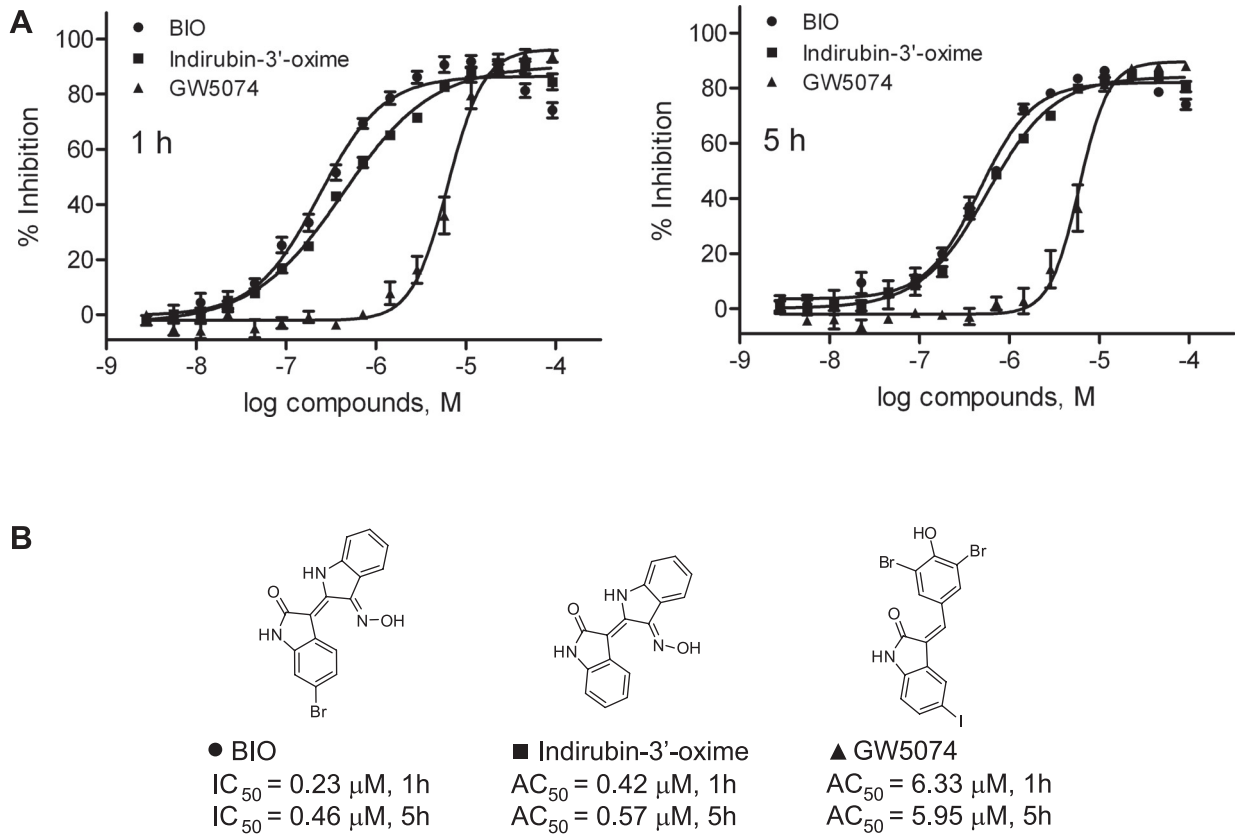

Fig. 5. 3′-Substituted indolone-related compounds. *A*: concentration response curves of (2′Z,3′E)-6-bromoindirubin-3′-oxime (BIO), indirubin-3′-oxime, and GW-5074 in Mito-MPS assay at 1 h (*left*) or 5 h (*right*) of treatment. *B*: structures of these compounds are shown with compound names, IC_{50} values in the Mito-MPS assay at 1 h or 5 h of treatment.

such as HeLa cells, but MMP changes cannot be detected in some other types of cells, including HepG2 and CHO cells as well as primary rat hepatocytes, due to its low S/B window (17). Therefore, this dye could not be used to accurately measure compound-induced MMP changes and efficiently evaluate the ability of compounds to induce mitochondrial toxicity.

In this study, we developed a homogenous cell-based assay using the Mito-MPS dye to evaluate changes in cellular MMP as a measure of mitochondrial toxicity. The Mito-MPS dye with membrane-permeable lipophilicity partitions between the cytoplasm and the mitochondria depending on the magnitude of MMP. The alteration of dye accumulation between the cytoplasm and the mitochondria indicates changes in MMP. This cell-based assay was easily miniaturized into a 1,536-well plate format and homogenously measured MMP changes with only one step of reagent addition. In addition, the ratiometric fluorescent readout from the dual emissions (590 and 535 nm) used in this assay minimizes the well-to-well and plate-to-plate variations caused by subtle differences in cell numbers and dispensing error.

The Mito-MPS dye was able to detect MMP changes by chemicals that affect different mitochondrial processes (Fig. 2, Table 2). The dye was able to detect changes produced by rotenone, an inhibitor of the NADH dehydrogenase; antimycin A, an inhibitor of the cytochrome c reductase; and FCCP and DNP, two uncouplers of MMP. These results make this dye a good first step in a potential strategy for assessing mitochondrial toxicity.

In the screening, we identified two interesting compound clusters, tyrphostins and 3′-substituted indolones, which decreased MMP. Tyrphostins were described as a group of small molecules that inhibit the phosphorylation of protein tyrosine kinases (PTK). These compounds were designed to compete with the substrate, but not with ATP, making them more selective and nontoxic PTK inhibitors (16). In addition to inhibiting tyrosine kinases, several tyrphostins, such as tyrphostin A9 (4, 26) and tyrphostin AG-126 (26), have also been found to decrease MMP in the cells, consistent with the findings from our current study. All of the tyrphostins, except for tyrphostin 1, decreased MMP in the HepG2 cells. The compound potency on inducing MMP changes appeared to depend on the presence of tertiary butyl (t-butyl) groups and the number of hydroxyl groups on the phenyl ring of the tyrphostins. The presence of t-butyl groups seemed to enhance compound potencies as seen in tyrphostins A9 (IC_{50} = 0.07 μM) and AG-879 (IC_{50} = 0.51 μM) from the primary screen (Supplemental Table S2). Tyrphostins 25 and 51 each with three hydroxyl groups were less potent or inactive at inducing MMP changes compared with the tyrphostins with two or fewer hydroxyl groups on the phenyl ring. As an exception, however, tyrphostin 1 with no hydroxyl group was inactive in the cells after 1 or 5 h of treatment.

Another interesting group of compounds that decreased MMP in HepG2 cells shared the indolone moiety; these included BIO, indirubin-3′-oxime, and GW-5074. Indirubin-3′-oxime is a cyclin-dependent kinase (CDK) inhibitor (3, 11). Previous studies show that indirubin and its derivates significantly decreased MMP and inhibited cell proliferation, which is unrelated to targeting CDK (18). Indirubin derivatives also caused G2/M phase cell cycle arrest and induced apoptosis via p53- and mitochondria-dependent pathways in human cancer cells (14, 30). Varela et al. (34) further studied the mechanisms of indirubin-3′-oxime toxicity on mitochondria. They found that indirubin-3′-oxime had direct effects on mitochondria function by disturbing MMP and impairing mitochondrial oxidative phosphorylation in isolated rat liver mitochondria. To our knowledge, other 3′-substituted indolone derivates including GW-5074, a c-Raf inhibitor (13), and BIO, a CDK inhibitor (23), have not been reported to disrupt MMP in HepG2 cells previously. However, the mechanism of action of these compounds on mitochondria needs to be further studied by investigating their effects on other mitochondrial activity end-points, such as oxygen consumption and reactive oxygen species production.

In summary, we have developed and validated a homogenous, cell-based MMP assay using the Mito-MPS dye in a 1,536-well plate format. The Mito-MPS dye was evaluated compared with JC-1, rhodamine 123, and TMRE and showed large dynamic windows in MMP changes in HepG2 cells. From the primary LOPAC library screening, we identified several known and novel compounds that decreased MMP. All of these compounds were also confirmed in an imaging-based assay. Our results indicate that this homogenous assay is suitable for the screening and profiling of large chemical libraries for their effects on mitochondrial function.

ACKNOWLEDGMENTS

We thank Darryl Leja for illustrations.

GRANTS

This research was supported by the Intramural Research Program (interagency agreement #Y3-ES-7020-01) of the Division of the National Toxicology Program, National Institute of Environmental Health Sciences, and the National Human Genome Research Institute, National Institutes of Health.

DISCLOSURES

No conflicts of interest, financial or otherwise, are declared by the author(s).

AUTHOR CONTRIBUTIONS

Author contributions: S.S., X.L., M.S.A.-R., J.L., L.S., and M.X. performed experiments; S.S., X.L., J.L., and M.X. drafted manuscript; X.L., R.R.T., and M.X. interpreted results of experiments; M.S.A.-R. and M.X. prepared figures; M.S.A.-R., R.H., J.L., R.R.T., and M.X. edited and revised manuscript; R.H., M.S.A.-R., and M.X. analyzed data; R.R.T., C.P.A., and M.X. approved final version of manuscript; M.X. conception and design of research.

REFERENCES

1. **Alberts B, Johnson A, Lewis J, Raff M, Roberts K, Walter P.** Energy conversion: mitochondria and chloroplasts. In: *Molecular Biology of the Cell*. New York: Garland Science, 2002, p. 767–829.
2. **Bassoe CF, Li N, Ragheb K, Lawler G, Sturgis J, Robinson JP.** Investigations of phagosomes, mitochondria, and acidic granules in human neutrophils using fluorescent probes. *Cytometry B Clin Cytom* 51: 21–29, 2003.
3. **Buolamwini JK.** Cell cycle molecular targets in novel anticancer drug discovery. *Curr Pharm Des* 6: 379–392, 2000.
4. **Burger AM, Kaur G, Alley MC, Supko JG, Malspeis L, Grever MR, Sausville EA.** Tyrphostin AG17, [(3,5-Di-tert-butyl-4-hydroxybenzylidene)-malononitrile], inhibits cell growth by disrupting mitochondria. *Cancer Res* 55: 2794–2799, 1995.
5. **Chan K, Truong D, Shangari N, O'Brien PJ.** Drug-induced mitochondrial toxicity. *Expert Opin Drug Metab Toxicol* 1: 655–669, 2005.
6. **Chaudhary PM, Roninson IB.** Expression and activity of P-glycoprotein, a multidrug efflux pump, in human hematopoietic stem cells. *Cell* 66: 85–94, 1991.

7. **Chazotte B.** Labeling mitochondria with fluorescent dyes for imaging. *Cold Spring Harb Protoc* 2009: pdb.prot4948, 2009.
8. **Ernster L, Dallner G, Azzone GF.** Differential effects of rotenone and amytal on mitochondrial electron and energy transfer. *J Biol Chem* 238: 1124–1131, 1963.
9. **Farkas DL, Wei MD, Febbroriello P, Carson JH, Loew LM.** Simultaneous imaging of cell and mitochondrial membrane potentials. *Biophys J* 56: 1053–1069, 1989.
10. **Hopfer U, Lehninger AL, Thompson TE.** Protonic conductance across phospholipid bilayer membranes induced by uncoupling agents for oxidative phosphorylation. *Proc Natl Acad Sci USA* 59: 484–490, 1968.
11. **Knockaert M, Greengard P, Meijer L.** Pharmacological inhibitors of cyclin-dependent kinases. *Trends Pharmacol Sci* 23: 417–425, 2002.
12. **Knowles BB, Howe CC, Aden DP.** Human hepatocellular carcinoma cell lines secrete the major plasma proteins and hepatitis B surface antigen. *Science* 209: 497–499, 1980.
13. **Lackey K, Cory M, Davis R, Frye SV, Harris PA, Hunter RN, Jung DK, McDonald OB, McNutt RW, Peel MR, Rutkowske RD, Veal JM, Wood ER.** The discovery of potent cRaf1 kinase inhibitors. *Bioorg Med Chem Lett* 10: 223–226, 2000.
14. **Lee JW, Moon MJ, Min HY, Chung HJ, Park EJ, Park HJ, Hong JY, Kim YC, Lee SK.** Induction of apoptosis by a novel indirubin-5-nitro-3′-monoxime, a CDK inhibitor, in human lung cancer cells. *Bioorg Med Chem Lett* 15: 3948–3952, 2005.
15. **Lenaz G, Bovina C, D'Aurelio M, Fato R, Formiggini G, Genova ML, Giuliano G, Merlo Pich M, Paolucci U, Parenti Castelli G, Ventura B.** Role of mitochondria in oxidative stress and aging. *Ann NY Acad Sci* 959: 199–213, 2002.
16. **Levitzki A.** Tyrphostins–potential antiproliferative agents and novel molecular tools. *Biochem Pharmacol* 40: 913–918, 1990.
17. **Lu J, Llorente I, Rohrer J, Li X.** A new fluorescent mitochondrial membrane potential sensor for imaging and fluorescence plate reader based applications. In: *SBS 14th Annual Conference & Exhibition*. St. Louis, MO, 2008.
18. **MacDonald ML, Lamerdin J, Owens S, Keon BH, Bilter GK, Shang Z, Huang Z, Yu H, Dias J, Minami T, Michnick SW, Westwick JK.** Identifying off-target effects and hidden phenotypes of drugs in human cells. *Nat Chem Biol* 2: 329–337, 2006.
19. **Marchetti P, Castedo M, Susin SA, Zamzami N, Hirsch T, Macho A, Haeffner A, Hirsch F, Geuskens M, Kroemer G.** Mitochondrial permeability transition is a central coordinating event of apoptosis. *J Exp Med* 184: 1155–1160, 1996.
20. **Mitchell P.** Coupling of phosphorylation to electron and hydrogen transfer by a chemi-osmotic type of mechanism. *Nature* 191: 144–148, 1961.
21. **Papkovsky DB, Hynes J, Will Y.** Respirometric screening technology for ADME-Tox studies. *Expert Opin Drug Metab Toxicol* 2: 313–323, 2006.
22. **Parascandola J.** Dinitrophenol and bioenergetics: an historical perspective. *Mol Cell Biochem* 5: 69–77, 1974.
23. **Polychronopoulos P, Magiatis P, Skaltsounis AL, Myrianthopoulos V, Mikros E, Tarricone A, Musacchio A, Roe SM, Pearl L, Leost M, Greengard P, Meijer L.** Structural basis for the synthesis of indirubins as potent and selective inhibitors of glycogen synthase kinase-3 and cyclin-dependent kinases. *J Med Chem* 47: 935–946, 2004.
24. **Ravagnan L, Roumier T, Kroemer G.** Mitochondria, the killer organelles and their weapons. *J Cell Physiol* 192: 131–137, 2002.
25. **Reers M, Smith TW, Chen LB.** J-aggregate formation of a carbocyanine as a quantitative fluorescent indicator of membrane potential. *Biochemistry* 30: 4480–4486, 1991.
26. **Sagara Y, Ishige K, Tsai C, Maher P.** Tyrphostins protect neuronal cells from oxidative stress. *J Biol Chem* 277: 36204–36215, 2002.
27. **Salvioli S, Ardizzoni A, Franceschi C, Cossarizza A.** JC-1, but not DiOC6(3) or rhodamine 123, is a reliable fluorescent probe to assess delta psi changes in intact cells: implications for studies on mitochondrial functionality during apoptosis. *FEBS Lett* 411: 77–82, 1997.
28. **Scaduto RC Jr, Grotyohann LW.** Measurement of mitochondrial membrane potential using fluorescent rhodamine derivatives. *Biophys J* 76: 469–477, 1999.
29. **Scorrano L, Petronilli V, Colonna R, Di Lisa F, Bernardi P.** Chloromethyltetramethylrosamine (Mitotracker Orange) induces the mitochondrial permeability transition and inhibits respiratory complex I. Implications for the mechanism of cytochrome c release. *J Biol Chem* 274: 24657–24663, 1999.
30. **Shi J, Shen HM.** Critical role of Bid and Bax in indirubin-3′-monoxime-induced apoptosis in human cancer cells. *Biochem Pharmacol* 75: 1729–1742, 2008.
31. **Slater EC.** The mechanism of action of the respiratory inhibitor, antimycin. *Biochim Biophys Acta* 301: 129–154, 1973.
32. **Sugrue MM, Wang Y, Rideout HJ, Chalmers-Redman RM, Tatton WG.** Reduced mitochondrial membrane potential and altered responsiveness of a mitochondrial membrane megachannel in p53-induced senescence. *Biochem Biophys Res Commun* 261: 123–130, 1999.
33. **Susin SA, Zamzami N, Castedo M, Hirsch T, Marchetti P, Macho A, Daugas E, Geuskens M, Kroemer G.** Bcl-2 inhibits the mitochondrial release of an apoptogenic protease. *J Exp Med* 184: 1331–1341, 1996.
34. **Varela AT, Gomes AP, Simoes AM, Teodoro JS, Duarte FV, Rolo AP, Palmeira CM.** Indirubin-3′-oxime impairs mitochondrial oxidative phosphorylation and prevents mitochondrial permeability transition induction. *Toxicol Appl Pharmacol* 233: 179–185, 2008.
35. **Wallace DC.** A mitochondrial paradigm of metabolic and degenerative diseases, aging, and cancer: a dawn for evolutionary medicine. *Annu Rev Genet* 39: 359–407, 2005.
36. **Xia M, Huang R, Sun Y, Semenza GL, Aldred SF, Witt KL, Inglese J, Tice RR, Austin CP.** Identification of chemical compounds that induce HIF-1alpha activity. *Toxicol Sci* 112: 153–163, 2009.
37. **Zamzami N, Marchetti P, Castedo M, Hirsch T, Susin SA, Masse B, Kroemer G.** Inhibitors of permeability transition interfere with the disruption of the mitochondrial transmembrane potential during apoptosis. *FEBS Lett* 384: 53–57, 1996.
38. **Zhang JH, Chung TD, Oldenburg KR.** A simple statistical parameter for use in evaluation and validation of high throughput screening assays. *J Biomol Screen* 4: 67–73, 1999.